Solar filaments - Comparing multi-wavelength observations with magnetic modelling

B. Schmieder

Observatoire de Paris, Section Meudon
92195 Meudon Cedex Principal, France

Abstract. Multi-wavelength observations of a filament/prominence obtained during campaigns with the space missions (SOHO, Yohkoh, TRACE) open a new research field. Physical conditions of filaments and their environment (i.e. temperature, dynamics, electron density) provides important constraints on theories of formation, stability or instability. The fine structures of filament are discussed in the framework of magnetic configurations: Is the prominence field a sheared arcade or a twisted flux rope? What is the magnetic structure of the footpoints of prominences called also "barbs"? Are the field lines dipped or are they vertical?

We present some new developments of 3-D models of a bipolar magnetic field and twisted flux tube which explain the fine structures in prominences as well as the feet. The new models bring valuable information on the global solar magnetic field with direct implications for dynamo theories and on the helicity of the heliosphere.

1. Introduction

Solar prominences are cool structures ($\sim 10^4$ K). They are visible in the hydrogen Hα line, visible as large and bright structures over the limb. On the disk they are dark filaments overlying the bright chromosphere. The understanding of their nature requires studies in multiwavelengths which allow to cover a large temperature range and to analyse the environment of the prominence. Since long ago these objects have been observed in Hα line. Let us mention Deslandres and Hale who built spectroheliographs by the end of the

19th century and the thesis of d'Azambuja and d'Azambuja (1948) which reported the main properties of filaments. Since that time, routine programs are performed i.e. the Meudon observations every day of the full disk in 3 wavelengths (Hα, Ca II K1, Ca II K3). In Hα and Ca II K3 we see respectively filaments on the disk and prominences at the limb (Figs. 1 and 2).

Progress has been achieved recently in prominences studies, with the development of high resolution telescopes and spectrographs on the ground (in Canaries Islands: THEMIS/MSDP, VTT/MSDP, LaPalma/SVST, in Ondrejov, in Bialkow, in Big Bear) and in space. We have a great opportunity with the launch of three space missions observing the Sun (Yohkoh since 1991, SOHO since 1996, TRACE since 1998). The instruments onboard the space missions observe in EUV lines and in soft X-rays. They are useful to study the transition region between the prominence and the corona and to detect the instability process leading to filament eruption and coronal mass ejection (CME).

In the next section I will review briefly the main properties of filaments, pointing out the problem of their formation (see book of Tandberg-Hanssen 1994). Then I will focus on the presentation of the magnetic field supporting the filaments against gravity and conclude by inserting prominences in a more global context relating them to the dynamo process below the photosphere on one hand and on the other end, to the large magnetic clouds approaching the Earth after CMEs.

	Quiescent Prominence	Remarks
length	60 - 600 Mm	less for active-region filament
wide	4 - 15 Mm	
distance between feet	30 Mm	size of the supergranules
density	10^{10} - 10^{11} cm^{-3}	less in prominence-corona region (10^8 - 10^9 in cavity)
temperature	5000 - 8000 K	higher T (PCTR) observed in UV lines
magnetic field	4 - 50 G	100 G in active-region prominence
angle (axis of prom./B)	15 - 25 degrees	Hanle effect
configuration	inverse	normal for active region filament
magnetic flux	2.5 $\times 10^{19}$ Mx	for active-region filament F = 10^{20} - 10^{21} Mx
flows	vertical 0.5 - 5 km/s, horizontal 10 - 20 km/s	60 km/s in active prominences
Diagnostics	Hydrogen lines (Hα - Lyman lines), Ca II radio $\lambda < 1$ cm	NLTE radiative transfer physical parameters (Nobeyama Observatory)

Table 1: Identity card of prominences.

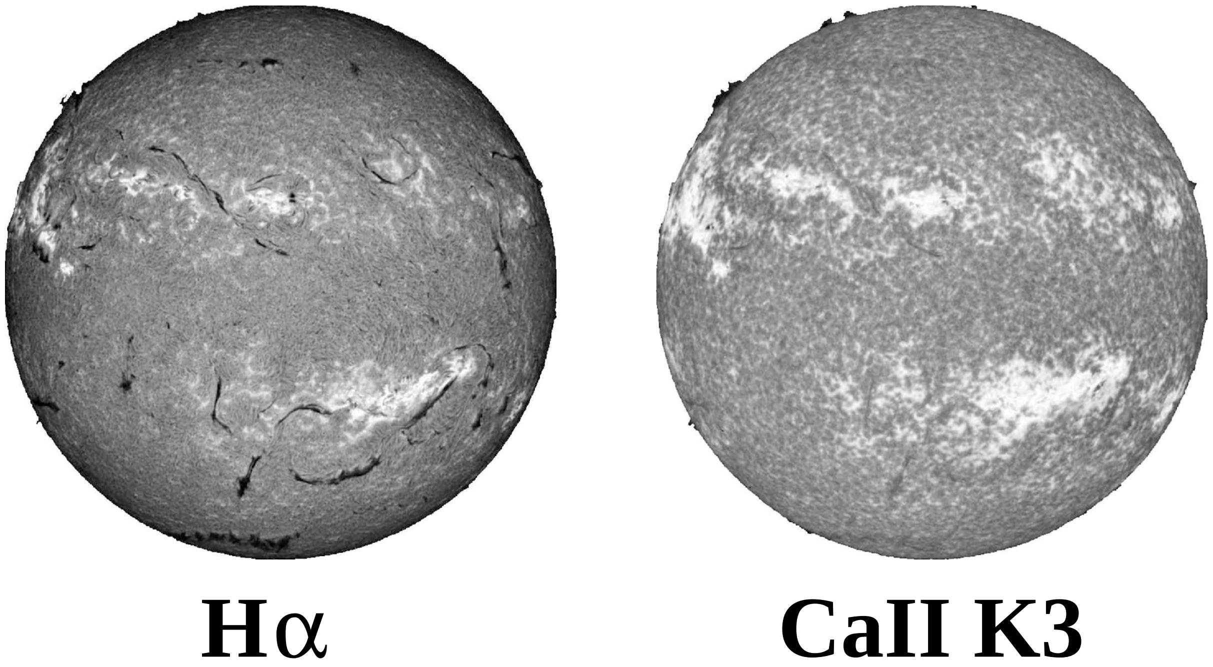

Figure 1: The chromosphere observed in the lines Hα of hydrogen and Ca K3 of ionized calcium as spectroheliograms obtained at Meudon. On the disk long dark structures are the filaments. Above the limb some dark prominences are well visible in K3. Bright areas correspond to plages. In K3 we see the regular network (Courtesy of the Observatoire de Paris).

2. Properties of filaments

Filaments have very specific characteristics in length and width; they are long (100Mm)- e.g. quiescent filament lying generally in the Quiet Sun or around the poles (polar-crown filaments) and short (10 Mm) and low lying inside active centers (Table 1). They lie over the inversion line of the photospheric longitudinal magnetic field component. The strength of the magnetic field can be weak on both sides of the inversion line: i.e. $\sim$ 100-200 G for quiescent filaments. The physical quantities of prominences are derived from the analysis of the spectral lines. Because prominences are formed by cool plasma ($\sim 10^4$K) they are mainly visible in optically thick lines (Hα, He 10830 Å) which require the resolution of the radiative transfer equations. The cool plasma absorbs the radiated light of the Sun and produces emissions at the same frequencies mainly by partial or complete radiative redistribution. At the limb we observe only the emission, on the disk we have to distinguish between the 2 processes and to take into account that the prominence is not completly optically thick. Sophisticated treatement have been performed using non LTE approach (Gouttebroze, Heinzel and Vial 1993). The SOHO/SUMER spectrograph has observed filaments and prominences in the Lyman series. Lyman lines show a central reversal in filaments due to the absorption of the radiation of the cool plasma.

The observations in coronal lines in wavelengths shorter than the cut-off of the Lyman continua of Hydrogen (< 911 Å) or He (< 550 Å), show dark areas at the locations of

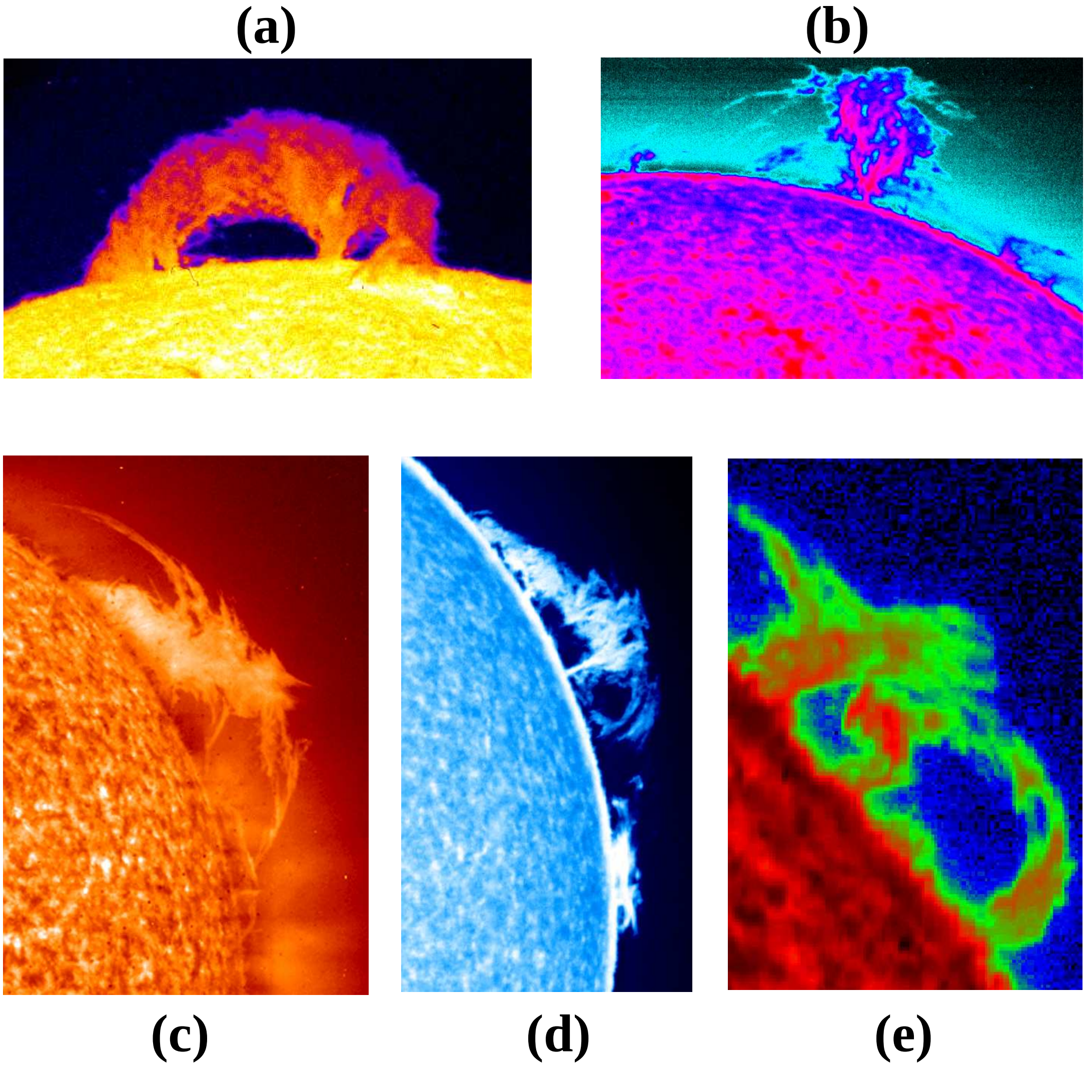

Figure 2: Observations of prominences in Hα (a), Ca II line (b) and (d) with the Meudon spectroheliograph in UV lines, (c) with EIT 304 Å and (e) with SUMER CIII line.

prominences. It is due to the absorption of this radiation (continua) by the cool plasma of the prominence. This phenomenon is well observed in coronal lines (Mg X) observed by SOHO/CDS spectrograph and by TRACE (171 Å and 195 Å) (Figure 3). Recent studies show that it is a good diagnostic to derive the hydrogen column density of the prominences (Kucera et al. 1998, Schmieder et al. 1999). The electron density is in fact difficult to estimate. Three orders of magnitude exist between the different determinations (10^9 to 10^{12} cm^{-3}). This discrepancy is due to the different methods of analysis or to the large variety of prominences or to the filling factor which is an unknown parameter.

The electron density is an important parameter because it is the clue to the interpretation of the stability of prominence. The scale height of a prominence is less than 500 km so it means that it is impossible to maintain plasma at 100 Mm high in a loop. Material will fall down immediately. This implies that the plasma pressure cannot provide the mechanism of support. So we need to consider other possible supports: dynamics, magnetic field or Alfvén waves.

The prominences observed as a whole object have a slow upflow of a few km/s and are relatively stable (Schmieder 1989, 1990). On a small scale it is nevertheless not true and the fibrils of filaments have longitudinal bidirectional flows (Fig. 4). That is difficult to undertand in a global approach (Schmieder et al. 1991, Zirker et al. 1998). So we have to consider seriously how the magnetic field supports the material (see next section). The instruments of SOHO (SUMER, EIT and CDS) are well adapted to observe the transition region betwen the filament and the corona (PCTR). EIT provides many movies of eruptive prominences in He II 304 Å (10^5 K) and shows how twisted are filaments as they erupt (Fig. 5).

In C IV and Si IV lines, the emission by the PCTR of filament is weak and difficult to be seen. Some fibrils were detected in filament channesl and were interpreted as legs of large loops overlying the prominences and heated by ohmic dissipation to 10^5 K temperature (Kucera et al. 1999). Statistical studies show that PCTR thickness is less than 100 km, which is under the spatial resolution of the instruments (Wiik et al. 1999).

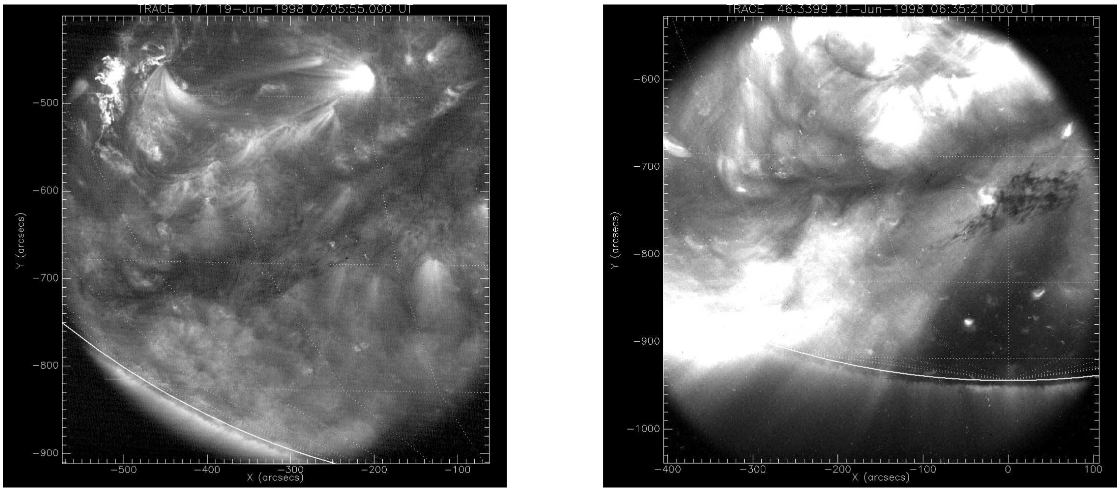

Figure 3: Polar crown filament observed with TRACE at 171 Å (left panel) on June 19 1998, (right panel) on June 21 1998. The filament is visible in the south of the filament channel because of perspective effects. The channel is dark because of lack of the coronal line emission, the filament is also dark because of the absorption of the coronal line by the cool plasma. North is up.

3. Magnetic field

3.1. Observations

3.1.1. Hanle effect

In prominences the Zeeman effect allows the measurement of the longitudinal component of the magnetic field (Kim 1990). Radio wavelengths provide information on the field

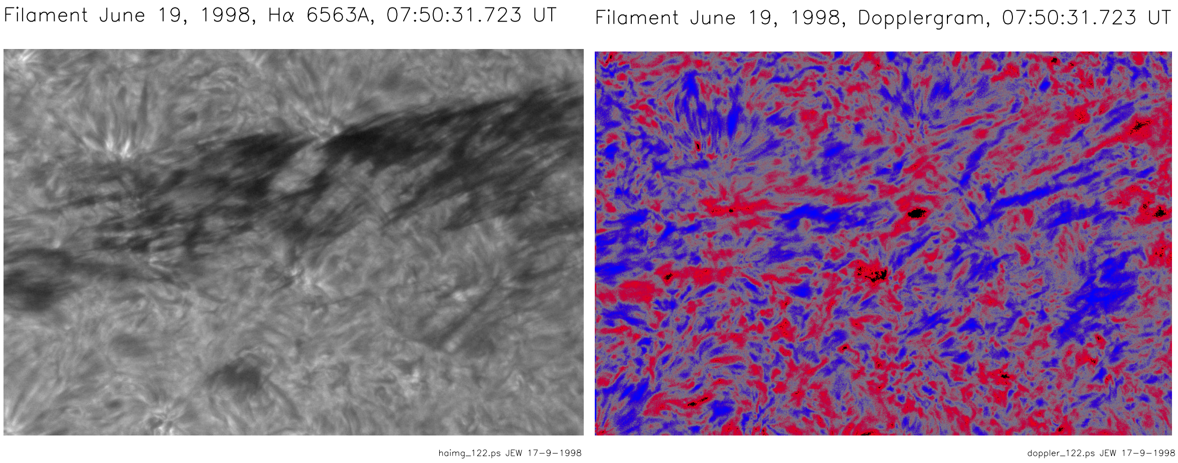

Figure 4: Polar crown filament observed in Hα on June 19 1998 by the SVST telescope in LaPalma ($100'' \times 250''$): (a) filament observed in Hα line center at 07:50:31 UT, (b) Doppler image derived from nearly simultaneous images recorded in H$\alpha \pm$ 0.25 Å. The North is more or less oriented towards the bottom of the image.

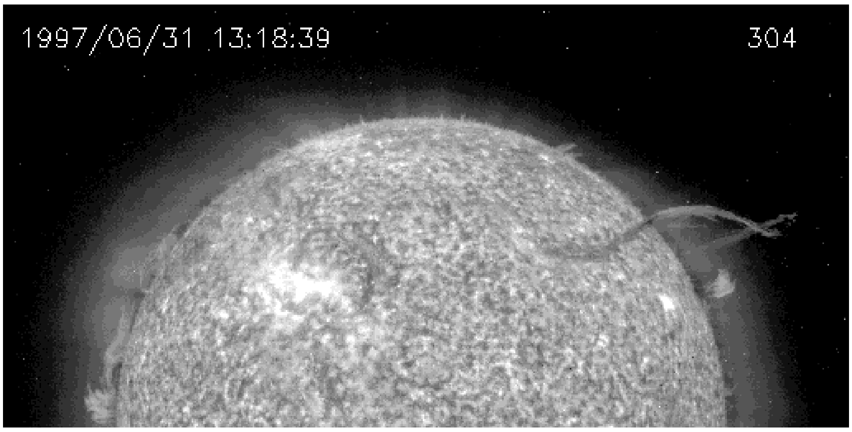

Figure 5: Eruptive twisted prominence observed by SOHO/EIT.

strength (Apushkinskii et al. 1990). The Hanle effect gives the three components of the field and the electron density from the polarization components in two spectral lines (Bommier et al. 1994). The main results of Hanle measurements are the following: the prominence field has the opposite direction to that expected from simple extrapolation of the photospheric field. It is called "Inverse type" (Leroy et al. 1984), contrary to the "Normal type" where the fields in prominences and photosphere have the same direction. 90% of prominences have the inverse type (Bommier et al. 1998). In that case the orthogonal component (B_{per}) is opposite to the field of a simple arcade and also the field component parallel to the prominence ($B_{//}$) is opposite to that of an arcade sheared by the differential rotation. The magnetic field in prominences is nearly horizontal field, homogeneous on the scale of a few arc seconds, and increasing with height (Leroy et al. 1983). The prominence fine structures are inclined by 20 to 30 degree towards the prominence main axis.

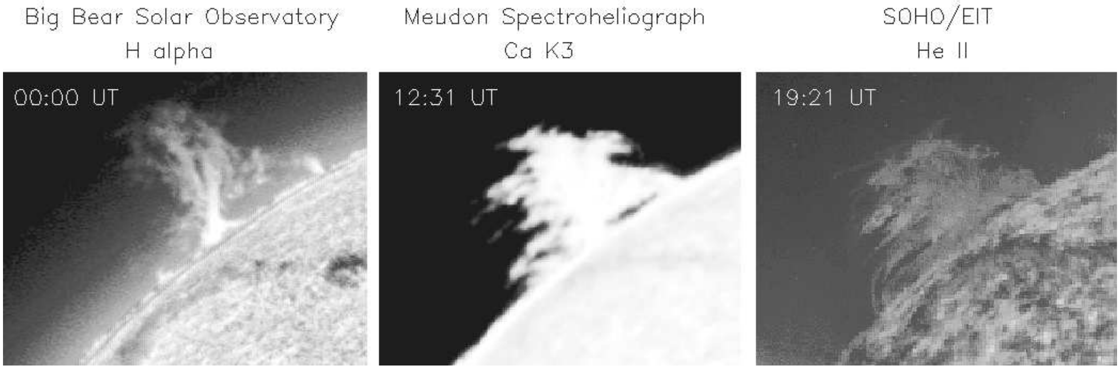

Figure 6: Example of a prominence observed in multi-wavelengths. It appears vertical in Hα and horizontal in He line.

3.1.2. Presence of magnetic dip

Let us assume that the cold material is supported by the magnetic field. If enough mass can be brought into the top of sheared magnetic arcade in less than one hour, the gravity force can bend the top of the field lines and form a dip (Dere et al. 1990, Fiedler and Hood 1993). The observations of dips are not evident but it could be suggested in some fine observations (Rompolt 1990). A long debate on the structures in prominences is still not clarified. Multi-wavelength observations show that prominence threads can appear vertical in Hα and horizontal in UV lines (Fig. 6). This has been explained as being due to the existence of long horiontal field lines, a part of them being heated to EUV temperatures while in the middle small dips are formed with cool plasma. Due to the perspective effect all the small dips in the different field lines could give the impression of the existence of a vertical structure (Aulanier et al. 1999, Kucera et al. 1999).

3.2. Magnetic configurations supporting prominences

Since the well known 2D model of Kippenhahn and Schlüter (1957), several models have been proposed in 2 1/2 D and then in 3D. Two types of models are considered: arcade-like configurations and twisted flux tubes.

3.2.1. Model in 3D with overlying arcade

Arcade models in 2 1/2 D cannot have a dip at the top of the field lines even when the magnetic shear increases (Amari et al. 1991). In 3D it can occur. The overlying arcade locally compresses the central part of an underlying sheared arcade (Antiochos et al. 1994). The latter model gives an inverse polarity prominence with a magnetic field nearly aligned with the photospheric inversion line. But the direction of the axial field will be wrong.

3.2.2. Quadrupolar configurations

These configurations naturally have a dip. Malherbe and Priest (1983) and later Démoulin and Priest (1993), Uchida (1998) developed such models. The presence of a corridor free of significant field is needed to have a prominence extension reaching the chromosphere and converging motions to provide mass. These models are perfectly adapted for active region filaments (Tang 1987) or filaments between two active regions (MacKay et al. 1998). The presence of "dual arcades" observed by Yohkoh/SXT might be a signature of magnetic reconnection in quadrupolar configurations (Uchida 1998).

3.2.3. Models in 3D with twisted flux tubes and "barbs"

This class of models provides the needed dipped magnetic field and seems to be well supported by recent observations. The twisted configuration can be obtained by photospheric twisting motions (Priest et al. 1989), by converging motions in a sheared arcade with magnetic reconnection at the inversion line (van Ballegooijen and Martens 1989), by resistive instability in a sheared arcade or by relaxation and accumulation of helicity (Démoulin and Priest 1989, Rust and Kumar 1994) or by emergence from the convective zone (Low 1994, 1996). Prominence feet appear as a direct consequence of the parasitic polarities present in the filament channel. Priest et al. (1996) used the emergence of small loops to create feet or "barbs". The feet would be due to the reconnection occurring between the emerging dipole and the main filament field. Aulanier and Démoulin (1998 a,b) showed that the feet appear naturally above secondary photospheric magnetic inversion lines produced by the parasitic polarities which create local quadrupolar configuration able to support the plasma in the feet.

3.2.4. 3D model of prominence with bald patch

A recent model has been developed by Aulanier et al. (1998c, 1999). These authors show the importance of field topology. They consider a bipolar configuration imposing a twisted flux tube by increasing the shear in the region. They use the equations of linear magnetohydrostatics (lmhs) for the extrapolation (Low 1992). Pressure and gravity are taken into account. They use directly the observed longitudinal fields, taken from magnetograms obtained by SOHO/MDI. They compare their field lines with the filament observations obtained on the ground (VTT, Tenerife) and in space (SUMER). They examine the dips of the field lines where material can be supported. They draw only the portion of the field lines dipped enough (2Mm). They find good agreement between the shape and location of the dipped field lines and the shape of the filament body (Fig. 7). MacKay et al. (1999) confirmed this model with a similar approach but using a relatively strong magnetic field bipole to represent the background which is not realistic for quiescent prominences.

4. Magnetic helicity and filaments

The observations show specific relationships of chirality among filaments, coronal arcades, active regions, coronal mass ejections and magnetic clouds.

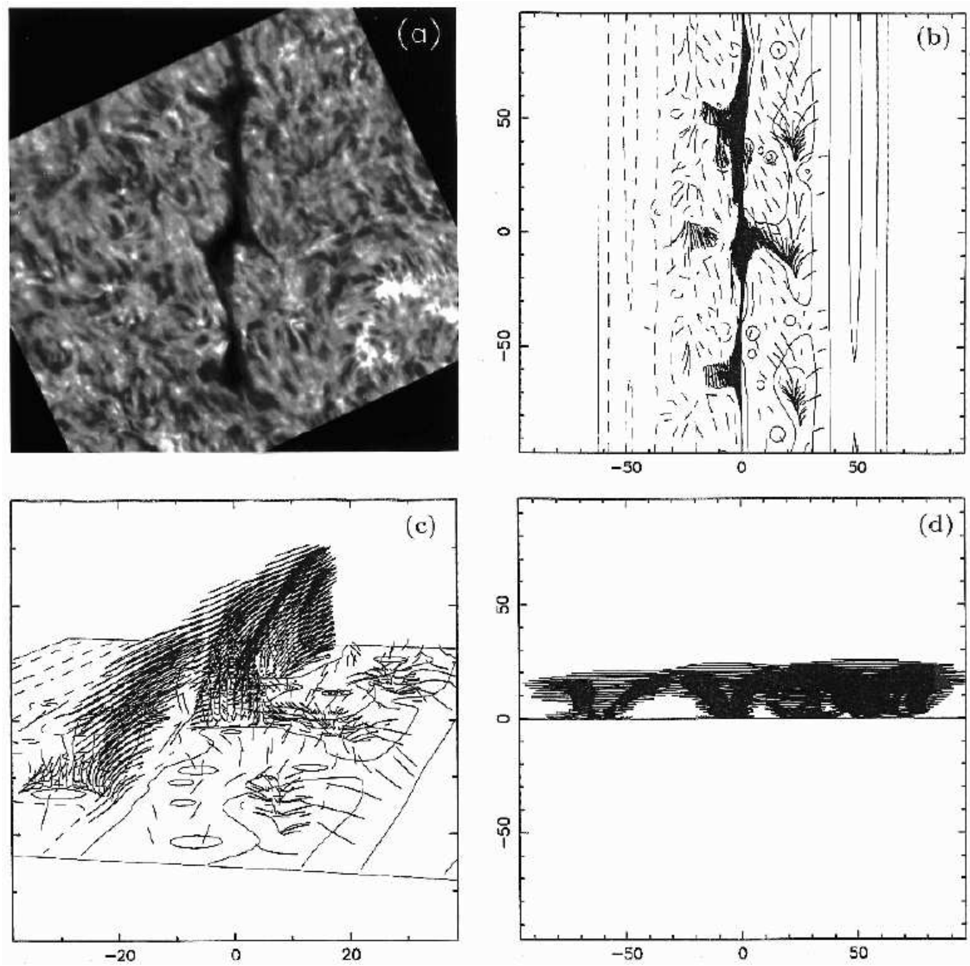

Figure 7: Model of bald patch filament in 3D: (a) Observations of a Hα filament with the MSDP spectrograph on the VTT at Tenerife, (b) MDI magnetogram and extrapolated magnetic field lines drawn only in the dips, (c) 3D view, (d) side view (Aulanier et al, 1998c).

4.1. Chirality of filament and fibrils

Filaments are always found above inversion lines of the photospheric magnetic field in regions, called corridors or filament channels, which are nearly free of chromospheric fibrils. They are also characterized on either side by the presence of Hα fibrils nearly aligned with the inversion line indicating a high magnetic shear (Foukal 1971, Rompolt 1990). The corridor is nearly free of vertical magnetic field flux except small parasitic polarities (Raadu et al. 1988, Martin 1990). At the locations of these small polarities we observed *the plagettes* from which fibrils stream parallel to the filament. Two morphological forms of filament channels and filaments have been identified. They are called *dextral and sinistral*. An observer standing on the positive polarity side of a dextral/sinistral filament would see the lateral feet pointing to the right/left along the filament channel.

For prominences these names correspond to right-bearing/left-bearing prominences if the prominence feet bear off to the right/left of the main axis of the prominence. All dextral filaments are right-bearing. Most quiescent filaments in the northern/southern hemisphere are *dextral/sinistral* at mid- and high latitudes, regardless of cycle (Martin et al. 1994, Martin and McAllister 1998). Observations show that there is a good correlation between the direction of the magnetic field along the filament as inferred from the plagettes and as inferred from the lateral prominence feet.

4.2. Coronal arcades

The X-ray observations made by Yohkoh/SXT have told much about the coronal arcades overlying filament channels (McAllister et al. 1998). The skew of the coronal arcades changes according to the hemisphere. Skew was defined as the acute angle between the loops and the polarity inversion or filament axis. If the arcade loops cross over the filament in the sense of threads of a left-hand/right-hand screw they defined the loops as left-skewed/right-skewed. Left skewed arcades overlie dextral filaments (Martin and McAllister et al. 1995).

4.3. Shear angle and sigmoids

Conspicuous fibrils are observed near sunspots penumbras. Richardson (1941), recognizing a similarity between fibril pattern and the pattern of iron fillings around bar magnets, made an extensive study of the orientation of the superpenumbra fibrils and found that the majority is clockwise for sunspots in the southern hemisphere. This was confirmed later by Rust and Martin (1994). On the other hand Seehafer (1990) estimated the electric current helicity in 16 active regions and concluded that the electric current helicity is predominantly positive/negative in the southern/northern hemisphere. This result was confirmed also from a comparison between Mees vector magnetograms and current-free configurations (Pevtsov et al. 1995).

Very large scale X-ray structures have been noticed to exhibit a slender S or backward-S shape as a function of hemisphere (Rust and Kumar 1994, Moore et al. 1997). Reverse S-shaped structures predominate in the northern hemisphere as do S-shaped structures in the southern hemisphere. In active regions such shape is called sigmoid, they are frequently observed in X-ray around the flare time showing strong shear (Rust and Kumar 1996, Canfield et al. 1999).

4.4. Twisted configurations

Filaments destabilize for different reasons. Emerging flux in filament channels can lead to disruption of the filament (Raadu et al. 1988). On the other hand they can be destabilized by some instabilities in the corona (Antiochos et al., 1999). Eruptive prominences appear commonly twisted (Fig. 5). Modeling a filament as an initially untwisted axial magnetic field aligned with the inversion field, Martin and McAllister (1998) claim that dextral filaments develop right-helical twist on the sun and that the corresponding interplanetary clouds have the helicity opposite to the CMEs after they have been detached from the Sun by reconnection. This solution is controversial and another solution of all these laws of chirality is proposed based on the idea that the filament lies in the lower portion of a large-scale helical magnetic field which supports the filament against gravity (Rust and Kumar 1994, Aulanier et al. 1998 c, 1999, MacKay et al. 1999).

4.5. Helical structure of magnetic cloud

Interplanetary clouds are the ejected parts of coronal mass ejections as first concluded by Marubashi (1986). Many such plasma clouds have helical structure detected by magnetometers on board spacecrafts (Burlaga 1991, Bothmer et al. 1996, Webb 1998). Gosling (1990) proposed that helical magnetic fields in interplanetary clouds originate from magnetic reconnection in ascending coronal arcades. Based on the same scenario, Martin and McAllister (1998) anticipate that left-skewed coronal arcades become left-helical CMEs and are detectable later as left-helical interplanetary clouds. Rust and Kumar (1994) found that the majority of interplanetary clouds with left/right-helical structures come from the northern/southern hemispheres, but they proposed that the helicity of the clouds reflects the helicity of the filaments before they erupt which in turn reflects the helicity of the solar dynamo generated fields.

5. Discussion on helicity

A natural way to explain how both magnetic field components, parallel and normal to the prominence, are inverse is to use a quadrupolar field sheared by the differential rotation (Priest et al. 1996). However, this gives a magnetic helicity dominance in each hemisphere opposite to observations. Van Ballegooijen et al. (1998) demonstrated that the differential rotation does not work correctly for the helicity conservation. Studying a switchback inversion line, they showed that the model taking into account the differential rotation predicts an opposite chirality on the 2 arms of the switchback which is contrary to the observations. Berger (1998) reviewed different statements that are well established to sketch a solution. Helicity is conserved in ideal MHD, and it is probably well conserved on the sun, so any positive helicity generated by plasma motions, for example, must be offset by negative helicity generation. Berger proposed to explain the sign of the helicity, namely, North hemisphere negative, South Hemisphere positive by taking into account the transfer of the helicity either into or from the solar wind or across the equator, beneath the surface. His solution to helicity in filaments is based on the emergence of twisted flux tubes. The same approach was advocated by Rust and Kumar (1994). Reconnection below the solar surface could create twisted flux tubes which emerge due to buoyancy. By transfer and redistribution of the helicity and by using faster rotation at the equator one can reproduce at least the observed global helicity pattern. Van Ballegooijen (1999) presented an MHD model which takes into account the solar differential rotation, the photospheric diffusion and flux cancellation in a 3D active region. After reconnection he formed a left/right helical flux rope in the North/South hemisphere from an untwisted emerging bipole.

Démoulin (1998) explained that the right sign of helicity could be obtained with Coriolis forces acting on diverging supergranular flows (Priest et al. 1989). This process is very efficient and can accumulate helicity in twisted tubes but since localized motions give neutralized currents, it is difficult to reproduce the dominance of one polarity as observed in each hemisphere.

If a local dynamo cannot give a good explanation, then global dynamo models should be investigated for their possible helicity-producing qualities (Seehafer 1998).

6. Conclusion

The large amount of data concerning helical features, from filaments to interplanetary clouds, have shown a great organizing principle of nature as originally pointed out by Rust (1994). We need models that can fit into a unified theory. We have shown the importance of twisted flux tube emergence, the presence of parasitic polarities in the inversion line corridor, the aligned fibrils in the filament corridor and all the chirality laws. Many questions are unsolved and we need further observations with multi-wavelength instruments to test the existing different proposed approachs.

References

Amari T., Démoulin P., Browning P., Hood A.W., Priest E.R. 1991, A&A, 241, 604

Antiochos S.K., Dahlburg R.B., Klimchuck J.A. 1994, ApJ, 420, L41

Antiochos S.K., DeVore C.R., Klimchuck J.A., 1999, ApJ, 510, 495

Anzer U. 1972, Solar Phys., 24, 324

Apushkinskii G.P., Nesterov N.S., Topchilo N.A., Tsyganov A.N. 1990, SvA, 34(5), 530

Aulanier G., Démoulin P., 1998a, Publications of the ASP, 150, 186

Aulanier G., Démoulin P., 1998b, A&A, 329, 1125

Aulanier G., Démoulin P., van Driel L., Mein P, deForest C. 1998c, A&A, 335, 309

Aulanier G., Démoulin P., Mein N., van Driel-Gesztelyi L., Mein P., Schmieder B. 1999, A&A, 342, 867

Berger M. 1998, Publications of the ASP, 150,102

Bommier V., Leroy J.L. 1998, Publications of the ASP, 150, 434

Bommier V., Landi Degl'Innocenti E., Leroy J.L., Sahal-Bréchot S., 1994, Solar Phys., 154, 231

Bothmer V., Desai M.I., Marsden R.G. et al. 1996, A&A, 316, 493

Burlaga L.F. 1991, in Physics of the Inner Heliosphere II, eds. R.Schwenn, E.Marsch, Springer Verlag, New York, 1

Canfield R., Hudson H., McKenzie D., 1999, Geophysical Research Letters, 26, 627

d'Azambuja L., d'Azambuja M. 1948, Annales de l'Observatoire de Paris, 6,7

Démoulin, P. 1998, Publications of the ASP, 150, 78

Démoulin P., Priest E.R. 1989, A&A, 214, 360

Démoulin P., Priest E.R. 1993, Solar Phys., 144, 283

Dere K.P., Schmieder B., Alissandrakis C. 1990, A&A, 233, 207

Fiedler R.A.S., Hood A.W. 1993, Solar Phys., 146, 297

Foukal P. 1971, Solar Phys., 19, 59

Gouttebroze P. Heinzel P., Vial J.C., 1993, Astron. and Astrophys. Suppl. Ser. 99, 513

Gosling J.T. 1990, in Physics of Magnetic Flux Ropes (eds) C.T.Russell, E.R. Priest, L.C.Lee, Geophys. Mono. Ser. 58, 343

Kim I.S. 1990, IAU Colloq. 117, Springer-Verlag, 49

Kippenhahn R., Schlüter A. 1957, Zs. Ap. 43, 36

Kucera T.A., Andretta V., Poland A.I. 1998, Solar Phys., 183, 107

Kucera T.A., Aulanier G., Schmieder B., Mein N. and J.C. Vial 1999, Solar Phys., 186, 259

Leroy J.L., Bommier V., Sahal-Bréchot S. 1983, Solar Phys., 83, 135

Leroy J.L., Bommier V., Sahal-Bréchot S. 1984, A&A, 131, 33

Low B.C. 1992, ApJ, 399, 300

Low B.C. 1994, Plasma Phys., 1, 1684

Low B.C. 1996, Solar Phys., 167, 217

MacKay D.H., Gaizauskas V., Ricckard G.J., Priest, E.R. 1998, ApJ, 486, 534

MacKay D.H., Longbottom A.W., Priest E.R., 1999, Solar Phys. 185, 87

McAllister A.H., Hundhausen A.J., MacKay D.H., Priest, E.R. 1998, Publications of the ASP, 150, 43

Malherbe J.M., Priest E.R. 1983, A&A, 123, 80

Marubashi K. 1997 in Coronal Mass ejections Geophys. Mono. Ser., 99, 147

Martin S.F. 1990, IAU Colloq. 117, Springer-Verlag, 1

Martin S.F., Bilimoria R., Tracadas P.W. 1994, in R. Rutten and C. Schrijvers (eds.), Solar Surface Magnetism, Kluwer Ac. Pub., 303

Martin S.F., Mc Allister A.H. 1995, in Proc. Colloq. IAU 153

Martin S.F., McAllister A.H. 1998, Publications of the ASP, 150, 419

Moore R.L., Schmieder B., Hathaway D.H., Tarbell T.D. 1997, Solar Phys., 176, 249

Pevtsov A.A., Canfield R.C., Metcalf T.R. 1995, ApJ, 440, L109

Priest E.R., Hood A.W., Anzer U. 1989, ApJ, 344, 1010

Priest E.R., Van Ballegooijen A.A., MacKay D.H. 1996, ApJ, 460, 530

Raadu M.A., Schmieder B., Mein N., Gesztelyi L. 1988, A&A, 197, 289

Richardson R.S. 1941, ApJ, 41, 24

Rompolt B. 1990, Hvar Obs. Bull. Vol. 14, 1, 37

Rust D.M. 1994, Geophys. Res. Lett. 21, 241

Rust D.M., Kumar A. 1994, Solar Phys., 155, 69

Rust D.M., Kumar A. 1996, ApJ, 464, L199

Rust D.M., Martin S.F. 1994, in Solar Active Region Evolution, Publications of the ASP 68, 337

Schmieder B. 1989, in E.R. Priest (ed.), *Dynamics and Structure of Quiescent Solar Prominences*, Kluwer Academic Publishers, Dordrecht, Holland, 15

Schmieder B. 1990, IAU Colloq. 117, Springer-Verlag, 85

Schmieder B., Kucera T., Heinzel P., Kotrč P. 1999, SPM meeting in Florence, ESA proceedings, SP-448, in press

Schmieder B., Raadu M.A., Wiik J.E. 1991, A&A, 252, 353

Seehafer N. 1990, Solar Phys., 125, 219

Seehafer N. 1998, Publications of the ASP, 150, 407

Tandberg-Hanssen E. 1994, the Nature of Solar Prominences, Kluwer Academic Publishers

Tang F. 1987, Solar Phys., 107, 233

Uchida Y. 1998, Publications of the ASP, 150, 163

van Ballegooijen A.A., Martens P.C.H. 1989, ApJ, 343, 971

van Ballegooijen A.A., Martens P.C.H. 1990, ApJ, 361, 283

van Ballegooijen A.A., Cartledge N.P., Priest E.R. 1998, Public. of the ASP, 150, 265

van Ballegooijen A.A., 1999, in Magnetic Helicity in Space and Laboratory Plasma, eds. Brown M.R., Canfield R.C., Pevtsov A.A. Geophys. Monogr. Ser., AGU Washington D.C., 213

Webb D. 1998, Publications of the ASP, 150, 463

Wiik J.E., Dammasch I., Schmieder B., Wilhelm K 1999, Solar Phys., 187, 405

Zirker J.B., Engvold O., Martin S.F., 1998, Nature, Vol 396, 440

Discussion

K.D. Leka: Two notes: The preference for active region helicity as a function of hemisphere is a weak relation at best, and it is not yet clear, given uncertainties in measurements, how well the relation really holds (see Leka, Solar Phys. 1999, 188, 3 and 21). Second comment: the hemispheric preference for filament handedness is for high latitude filaments only. Martin et al. found little or no relation for active region filaments. This, of course relates to comment (1) above.

B. Schmieder: On small scale it is difficult to derive only one value of shear for aportion of an active region but on a global point of view and integrated in time (several rotations) it seems that an active region conserves a specific helicity. Seehafer and more recently L.van Driel demonstrated this statement.

S. Antiochos: The differential rotation will inject helicity into the corona. Is this not enough to explain the observed helicity?

B. Schmieder: It could be a good idea to think about the differential rotation, but it appears that it leads to a magnetic helicity dominance in each hemisphere opposite to the observations.

Zs. Kővári: I wonder about the average lifetime of these prominences. Does the lifetime change with the size, are these properties correlated?

B. Schmieder: The lifetime of a prominence can reach few rotations (until 7 months). We distinguish two class of prominences in and outside active regions (see Table 1).